JACS
JOURNAL OF THE AMERICAN CHEMICAL SOCIETY
Communication
pubs.acs.org/JACS

Dynamics of Inter-DNA Chain Interaction of Photoresponsive DNA

Yusuke Nakasone,[§] Hideaki Ooi,[†] Yukiko Kamiya,[†,‡] Hiroyuki Asanuma,[†] and Masahide Terazima*[,§]

[§]Department of Chemistry, Graduate School of Science, Kyoto University, Kyoto 606-8502, Japan

[†]Department of Molecular Design and Engineering, Graduate School of Engineering and [‡]Division of Materials Research, Institute of Materials and Systems for Sustainability, Nagoya University, Nagoya 464-8603, Japan

Supporting Information

ABSTRACT: Photoresponsive DNA modified with azobenzene is an attractive design molecule for efficient photoregulation of DNA hybridization, which may be used for controlling DNA functions. Although the essential step of photocontrolling DNA is the initial isomerization of the azobenzene, the dissociation/association kinetics remain unknown. Here, the time-resolved diffusion method was used to trace the dissociation/association processes of photoresponsive DNA. Although the isomerization of azobenzene occurs in picoseconds, the dissociation of the double-stranded DNA to single-stranded DNA triggered by the *trans* to *cis* isomerization takes place ~10^7 times slower, with a time constant of 670 μs at 200 μM. From the concentration dependence, the dissociation and association rates were determined. Furthermore, the reaction rate from the single- to double-stranded DNA after the *cis* to *trans* isomerization was measured to be 3.6 ms at 200 μM. The difference in the melting temperatures of DNA between tethered *trans*- and *cis*-azobenzene is explained by the different rate of dissociation of the double-stranded form.

Photoresponsive DNA modified with azobenzene has attracted significant attention for its potential in controlling DNA functions, nanomachines, and nanocapsules by light.[1−9] The azobenzenes are incorporated into DNA sequences by tethering them to sugar/phosphate linkages along the DNA backbone via a D-threoninol group (azo-DNA).[10,11] Although the *trans*-form in the DNA sequence (azo^{trans}-DNA) stabilizes the DNA duplex (d-azo^{trans}-DNA) by intercalation between the neighboring bases, the *cis*-form (azo^{cis}-DNA) destabilizes the duplex (d-azo^{cis}-DNA), owing to a steric constraint.[10−14] Thus, hybridization of DNA by light is possible by using these reactions of azobenzene.[10−12]

The essential step of photocontrolling DNA is the initial isomerization of the azobenzene and subsequent association/dissociation (A/D) of the DNA duplex. The well-characterized isomerization reaction of azobenzene is known to take place within 20 ps.[15] The question that remains is how fast are the subsequent dissociation and association processes of DNA after this isomerization? Since dissociation of the DNA duplex is induced by steric repulsion between the *cis* azobenzene and DNA base pairs, it is plausible that the dissociation occurs very fast. However, the dynamics of duplex formation and dissociation triggered by the isomerization have not been clarified because there is no time-resolved method that traces the intermolecular interaction change. For example, although the A/D may be monitored as a change in absorbance at 260 nm caused by the hyperchromic effect, such measurement would be difficult owing to two reasons. First, an expected absorption change could be very small, because the quantum yield of the reaction is very low, as shown in this study. Second, even if the small absorption change could be detected, the absorption change reflects only local changes around the bases, and it may not reflect the A/D process of the whole DNA chain. Thus, probing the A/D dynamics by different way is necessary. We have developed a new time-resolved method to monitor A/D in the time domain. This is based on the time-resolved measurement of the diffusion coefficient (D) by the transient grating (TG) method, which can trace time development of a molecular concentration pattern created by photoexcitation of a pair of laser pulses.[16] This technique is highly sensitive, because solely photoinduced changes can be detected without contributions from unreacted species. Furthermore, by monitoring the change in D, we can determine the A/D rate unambiguously, as previously demonstrated for several photosensor proteins.[17−21] Here, we applied this technique to trace the interaction change of a DNA duplex. The determination of the rate constants of A/D is important for understanding how the azobenzene perturbs the stability of the duplex and for evaluating the response time of the DNA nanomachines or regulating intermolecular interaction dynamics between DNA and transcriptional factors. This is the first detection of the dynamics of photoresponsive DNA.

Here, we measured the A/D rates of d-azo^{trans}-DNA as well as d-azo^{cis}-DNA. The sample preparation and experimental methods of the TG measurement are described in the SI, section SI-1. The equilibrium constants in the steady state were measured by monitoring the absorbance at 240 nm (Agilent, 8453) as a function of temperature. The melting curves (Figure S2) were analyzed by a sigmoidal function, and the fraction of the single-stranded and the double-stranded forms were determined. Using the fraction and the azo-DNA concentration, we calculated the concentration of double-stranded (dsDNA) and single-stranded (ssDNA) forms at each temperature at 10, 30, and 75 μM (SI-2). The equilibrium constants $K = [\mathrm{dsDNA}]/[\mathrm{ssDNA}]^2$ for the *cis*- and *trans*-forms (K^{cis} and K^{trans}, respectively) at 55 °C were determined to be 9.8×10^3 and 6.0×10^4 M^{-1}, respectively.

The dynamics after photoexcitation of d-azo^{trans}-DNA was investigated initially. The TG signals after UV excitation at 55 °C are shown in Figure 1a (SI-3 for a wider time range at $q^2 = 4.0 \times$

Received: March 8, 2016
Published: July 13, 2016

DOI: 10.1021/jacs.6b02525
J. Am. Chem. Soc. 2016, 138, 9001−9004

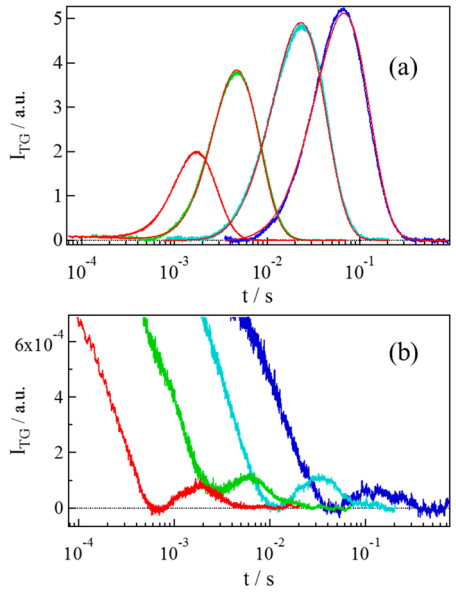

Figure 1. Molecular diffusion signals after photoexcitation of (a) d-azo^{trans}-DNA and (b) azo^{trans}-DNA at several grating wavenumbers (q^2 = 4.0×10^{12}, 1.5×10^{12}, 2.4×10^{11}, 6.3×10^{10} m^{-2} from left to right). The best-fitted curves based on the two-state model are shown as solid red lines in (a).

10^{12} m^{-2}). Immediately following excitation, the signal rose with the time response of our system (20 ns) and decayed single exponentially with a rate constant of $D_{th}q^2$, where D_{th} is the thermal diffusivity and q is the grating wavenumber. Hence this signal is attributed to the thermal grating signal. After this, the signal exhibited a rise-decay signal without reaching the baseline and finally decayed to the baseline. Since the time ranges of the rise-decay signals in the slower time region are dependent on the q^2 value (Figure 1a), the signal represents translational diffusion processes.

If the reaction completes in the signal observation time range, the TG signal is expressed as[16]

$$I_{TG}(t) = \alpha\{\delta n_{th}(t) + \delta n_P \exp(-D_P q^2 t) - \delta n_R \exp(-D_R q^2 t)\}^2 \quad (1)$$

where α is a constant, and δn_{th} is the thermal grating, and δn_R and δn_P are the refractive index changes due to the reactant and product, respectively. Since the sign of δn_{th} is negative at this temperature, we determined that the signs of the refractive index change of the rise and decay components were positive and negative, respectively, for d-azo^{trans}-DNA. Hence, the rise and decay components of d-azo-DNA are attributed to the diffusion of product and reactant (d-azo^{trans}-DNA), respectively. The product of the photoreaction diffuses faster than the reactant ($D_R < D_P$). This faster diffusion of the photoproduct is attributed to the d-azo^{cis}-DNA and subsequent product.

To examine the effect of isomerization to D of azobenzene, the TG signal of the single-stranded azo^{trans}-DNA (i.e., without the complementary strand (c-DNA)) under the same conditions was measured and is shown in Figures 1b and S4 for comparison purposes. The signal was almost identical until the decay of the thermal grating signal. After the thermal grating, the signal decayed once to the baseline, and the diffusion signal appeared, indicating that the signs of the refractive index change for the rise and decay components are opposite to those of d-azo^{trans}-DNA; i.e., the rise and decay signals were attributed to the molecular diffusion processes of the reactant (azo^{trans}-DNA) and the photoproduct (azo^{cis}-DNA), respectively. The faster rate of the rising component than that of the decay indicates that the product diffuses slower than the reactant ($D_R > D_P$).

The time development of molecular diffusion signals was obtained from the signals measured at several q^2 values (Figure 1). In the case of azo^{trans}-DNA (Figure 1b), the peak intensity did not depend on q^2, indicating that the D change completed in a fast time regime. Thus, isomerization of azobenzene completes within an ultrafast time scale (~20 ps). The temporal profile of the diffusion peak was well reproduced by a biexponential function (eq 1; without reaction kinetics), and D_R and D_P were determined to be $(3.6 \pm 0.1) \times 10^{-11}$ and $(3.5 \pm 0.1) \times 10^{-11}$ m^2/s, respectively. The D-change was very minor, and this is responsible for the weak intensity of the diffusion peak. We speculate that the isomerization of azobenzene perturbs the local conformation of the DNA, which leads to changes in the shape of the DNA and/or intermolecular interaction with solvent to decrease D slightly. The above measurement indicates $D_R > D_P$ for the azo^{trans}-DNA reaction. Hence, the observed $D_R < D_P$ for the d-azo^{trans}-DNA reaction is attributed to the dissociation of the dsDNA after the isomerization reaction.

Contrary to the case of azo^{trans}-DNA, the diffusion signal intensity of d-azo^{trans}-DNA depended on q^2 drastically (Figure 1a); the signal intensity increased with increasing the observation time range from a few milliseconds to seconds. This behavior is qualitatively explained as follows: On a short time scale, the diffusion signal intensity was weak, because the change in D for the product is small at this time ($D_P \approx D_R$), and the second and the third terms in eq 1 canceled. With increasing time, D_P gradually increased because of the dissociation reaction, and the difference between D_P and D_R increased, so that the diffusion peak intensity increased. The signal is quantitatively analyzed based on a model of $R \xrightarrow{h\nu} I \xrightarrow{k} P$, (a "two state model" (SI-1d). The expression for describing this reaction is given by[16]

$$I_{TG}(t) = \alpha\Bigg[\delta n_I \exp(-(D_I q^2 + k)t) + \delta n_P\Bigg[\frac{k}{(D_P - D_I)q^2 - k}\{\exp(-(D_I q^2 + k)t) - \exp(-D_R q^2 t)\}\Bigg] - \delta n_R \exp(-D_R q^2 t)\Bigg]^2 \quad (2)$$

where δn_I and D_I are the refractive index changes due to the I species and D of the intermediate, respectively.

In order to reduce the number of adjustable parameters in eq 2, D_R and D_P were initially determined. The diffusion signal obtained at $q^2 = 6.3 \times 10^{10}$ m^{-2} was reproduced by the biexponential function (eq 1), which indicates that the reaction kinetics did not overlap the diffusion signal. In other words, D was almost time independent over the time range of 20−300 ms. From the fitting, D_R and D_P were determined to be $(2.8 \pm 0.1) \times 10^{-11}$ and $(3.5 \pm 0.1) \times 10^{-11}$ m^2/s, respectively. This D_P value was the same as that of the product of azo^{trans}-DNA (i.e., azo^{cis}-DNA), indicating that the photoproduct is the single-stranded azo^{cis}-DNA. Using these parameters, the observed TG signals were reproduced very well over a wide time range from 100 μs to 1 s using a single reaction rate, k. The time constant of the change determined by the fitting was 670 μs at 200 μM. The D_I value was determined to be $(2.8 \pm 0.1) \times 10^{-11}$ m^2/s. The D change associated with the isomerization was not clearly observed. This may be because the conformational change observed in ssDNA

DOI: 10.1021/jacs.6b02525
J. Am. Chem. Soc. 2016, 138, 9001−9004

was suppressed by the formation of dsDNA and/or the weak D change was masked by the following strong D change.

The rate constant of the D change obtained above corresponds to the rate of relaxation after the equilibrium jump upon *trans*-to-*cis* isomerization. Since the rate constant of relaxation can be expressed as a sum of rates of forward and backward reactions in equilibrium[22] and the ratio between the rates is equal to the equilibrium constant K^{cis} (9.8×10^3 M^{-1}), we can calculate separately the rate of association (k_1^{cis}) and dissociation (k_{-1}^{cis}) (SI-1e). The k_1^{cis} and k_{-1}^{cis} were determined to be 9.8×10^6 M^{-1} s^{-1} and 1.0×10^3 s^{-1}, respectively.

We also investigated the formation process of the duplex (d-azo^{trans}-DNA) induced by the *cis*-to-*trans* isomerization of azo^{cis}-DNA in the presence of c-DNA. The sample solution was illuminated with UV LED (365 nm) to accumulate the *cis*-form of azobenzene. Under our experimental conditions, 70% of azobenzene was converted to the *cis*-form. The thermal diffusion and molecular diffusion signals were observed (Figure S5). From the sign of the refractive index change, the rise and decay components are assigned to the diffusion of reactant and product, respectively. For comparison, the TG signal after photoexcitation of azo^{cis}-DNA in the absence of c-DNA is shown in Figure S5. The rise and decay components are attributed to the diffusion of product and reactant, respectively.

Figure 2 shows the time development of molecular diffusion signals observed at several q^2 values. As the case of UV excitation,

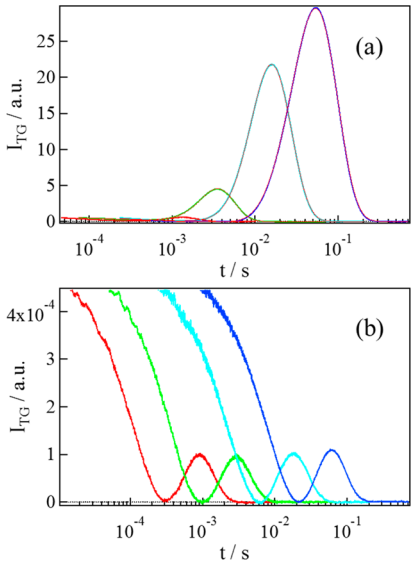

Figure 2. Molecular diffusion signals after photoexcitation of (a) d-azo^{cis}-DNA and (b) azo^{cis}-DNA at several grating wavenumbers ($q^2 = 4.9 \times 10^{12}$, 1.5×10^{12}, 2.4×10^{11}, 6.4×10^{10} m^{-2} from left to right). The best-fitted curves based on the two-state model are shown in solid red lines in (a).

the peak intensity of azo^{cis}-DNA did not depend on q^2, indicating that the D change completed in a fast time region as reported (Figure 2b). D_R and D_P were determined to be $(3.5 \pm 0.1) \times 10^{-11}$ and $(3.6 \pm 0.1) \times 10^{-11}$ m^2/s, respectively.

In the case of d-azo^{cis}-DNA, the signal intensity increased with increasing the observation time range (Figure 2a). The signals were analyzed based on the two-state model (eq 2). Using $D_R = (3.5 \pm 0.1) \times 10^{-11}$ and $D_P = (2.8 \pm 0.1) \times 10^{-11}$ m^2/s, which are obtained by fitting the diffusion signal at $q^2 = 2.1 \times 10^{10}$ m^{-2} with a biexponential function, the observed TG signals were reproduced very well over a wide observation time range with k. The time constant of the D change determined from the fitting was 3.6 ms. The D_I value was determined to be $(3.5 \pm 0.1) \times 10^{-11}$ m^2/s. Using the rate constant of relaxation after the equilibrium jump upon *cis*-to-*trans* isomerization and the equilibrium constant K^{trans}, we calculated the rate of association (k_1^{trans}) and dissociation (k_{-1}^{trans}) in equilibrium to be 2.7×10^6 M^{-1} s^{-1} and 45 s^{-1}, respectively. Analyzing the signals by the two-state model (eq 2), k was determined as a function of concentration of single strand c-DNA (SI-5).

Considering that the isomerization of the azobenzene takes place within tens of picoseconds,[15] it may be expected that repulsion also appears in this time range, because repulsion is a short-range interaction. Hence, the break of the base pair beside the azobenzene could be fast. On the contrary to this expectation, the dissociation time constant (670 μs) of whole DNA chains is very slow when compared with that of the isomerization rate. The present result indicates that the initial impact of the isomerization of azobenzene does not cause dissociation, but the steric strain is absorbed as strain in base pairs within other parts of the DNA molecules. Dissociation proceeds gradually owing to this strain.

The second-order rate constants of duplex formation k_1 (2.7×10^6 M^{-1} s^{-1} for the *trans*-form and 9.8×10^6 M^{-1} s^{-1} for the *cis*-form) are much smaller than the diffusion-limited reaction rate calculated from D of ssDNA (>10^9 M^{-1} s^{-1}).[23] This small k_1 suggests a very small steric factor; i.e., the duplex formation occurs only at a specific relative orientation of two single strands. This is reasonable, because matching with the complementary sequence is required for duplex formation. Former studies on the reaction rates of duplex formation for 12-mer oligonucleotides have reported comparable values ($k_1 = 0.20$–2.7×10^6 M^{-1} s^{-1} at 15–35 °C) to those obtained in this study.[24−28] Interestingly, the association rate of the *cis*-form is about 3.6 times faster than that of the *trans*-form. This faster rate may be explained as follows: The main energy barrier for the association reaction may come from the intercalation process of the azobenzene moiety among the bases of DNA. If this is the case, then it is expected that this energy barrier is smaller for the *cis*-form, because the bended part of the azobenzene moiety is not necessarily intercalated. The dissociation reaction rate was also increased by the isomerization of azobenzene from the *trans* to *cis* more dramatically ($k_{-1}^{trans} = 45$ and $k_{-1}^{cis} = 1.0 \times 10^3$ s^{-1}). Hence, the decrease of the melting temperature upon the *trans*-to-*cis* isomerization of azobenzene is attributed to the increase of the dissociation rate. It has been reported that, when a mismatched base pair is inserted in DNA, k_1 decreases and k_{-1} increases (but still very slow), and therefore the binding constant decreases.[29] In case of azobenzene insertion, however, both k_1 and k_{-1} increase upon isomerization from *trans* to *cis*-form, which indicates that the *cis*-form is better than *trans*-form at both association and dissociation. We conclude that the *cis*-form dissociates rapidly enough to overwhelm its relatively fast association.

The ratio of D of dsDNA (e.g., d-azo^{trans}-DNA) to that of ssDNA (e.g., azo^{trans}-DNA) was ~0.8. According to the Stokes–Einstein relationship, under a given environment (T and η), D reflects the molecular size.[30,31] If the difference in D between the duplex and the single-strand is interpreted in terms of a difference in the molecular radius, the molecular volume of the duplex would be $(1/0.8)^3 = 1.95$ times larger than that of the single-strand, which is a very reasonable estimation if only the size is taken into account. This result was initially unexpected, because dsDNA and ssDNA may possess very different intermolecular

DOI: 10.1021/jacs.6b02525
J. Am. Chem. Soc. 2016, 138, 9001−9004

interactions with the solvent, which should affect the diffusion process. The present result may imply that ssDNA has a rather spherical shape due to the loss of base stacking formed in the duplex. Schematic illustration of the photoresponsive DNA clarified in this study is depicted in Figure 3.

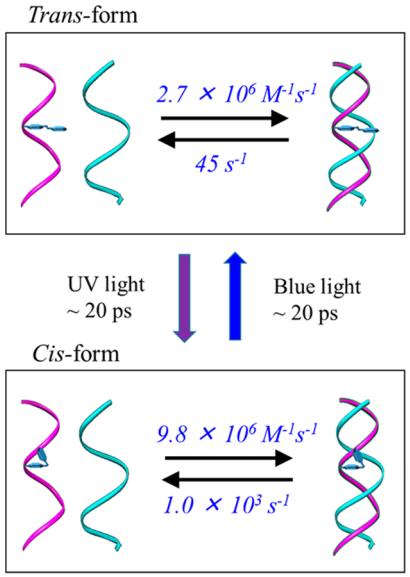

Figure 3. Schematic illustration of the dissociation and association reactions clarified in this study.

When we compared the TG signals between d-azo^{trans}-DNA and azo^{trans}-DNA (Figure S7), it should be noted that the signal intensities between the thermal grating and diffusion signal are significantly different. This difference can be explained by the quantum yield of *trans*-to-*cis* isomerization depending on the nature of DNA, ssDNA, or dsDNA, as reported.[32] On the basis of the analysis described in SI-6, we found that the quantum yield of *trans*-to-*cis* isomerization of azobenzene inserted into dsDNA was 3.6 times as large as that in ssDNA.

As the dissociation reaction can be triggered at a specific position by inserting azobenzene, we will investigate the molecular mechanism of association and dissociation (e.g., verify a zippering model)[33,34] by changing the sequence of DNA and number and position of the inserted azobenzene.

■ ASSOCIATED CONTENT

Supporting Information

The Supporting Information is available free of charge on the ACS Publications website at DOI: 10.1021/jacs.6b02525.

Experimental details and data (PDF)

■ AUTHOR INFORMATION

Corresponding Author

*mterazima@kuchem.kyoto-u.ac.jp

Notes

The authors declare no competing financial interest.

■ ACKNOWLEDGMENTS

This work was supported by Grants-in-Aid for Scientific Research (25288005 to M.T.) and a Grant-in-Aid for Scientific Research on Innovative Areas (Research in a proposed research area) (20107003, 25102004 (to M.T.), and 26102518 (to Y.K.)) from the Ministry of Education, Culture, Sports, Science and Technology of Japan.

■ REFERENCES

(1) Liu, M.; Asanuma, H.; Komiyama, M. *J. Am. Chem. Soc.* **2006**, *128*, 1009.
(2) Liang, X.; Nishioka, H.; Takenaka, N.; Asanuma, H. *ChemBioChem* **2008**, *9*, 702.
(3) Zhou, M.; Liang, X.; Mochizuki, T.; Asanuma, H. *Angew. Chem., Int. Ed.* **2010**, *49*, 2167.
(4) Takenaka, T.; Endo, M.; Suzuki, Y.; Yang, Y.; Emura, T.; Hidaka, K.; Kato, T.; Miyata, T.; Namba, K.; Sugiyama, H. *Chem. - Eur. J.* **2014**, *20*, 14951.
(5) Yuan, Q.; Zhang, Y.; Chen, T.; Lu, D.; Zhao, Z.; Zhang, X.; Li, Z.; Yan, C.-H.; Tan, W. *ACS Nano* **2012**, *6*, 6337.
(6) Li, J.; Wang, X.; Liang, X. *Chem. - Asian J.* **2014**, *9*, 3344.
(7) Liang, X.; Zhou, M.; Kato, K.; Asanuma, H. *ACS Synth. Biol.* **2013**, *2*, 194.
(8) Endo, M.; Yang, Y.; Suzuki, Y.; Hidaka, K.; Sugiyama, H. *Angew. Chem., Int. Ed.* **2012**, *51*, 10518.
(9) Kamiya, Y.; Asanuma, H. *Acc. Chem. Res.* **2014**, *47*, 1663.
(10) Asanuma, H.; Takarada, T.; Yoshida, T.; Tamaru, D.; Liang, X.; Komiyama, M. *Angew. Chem., Int. Ed.* **2001**, *40*, 2671.
(11) Nishioka, H.; Liang, X.; Kato, T.; Asanuma, H. *Angew. Chem., Int. Ed.* **2012**, *51*, 1165.
(12) Asanuma, H.; Ito, T.; Yoshida, T.; Liang, X.; Komiyama, M. *Angew. Chem., Int. Ed.* **1999**, *38*, 2393.
(13) Asanuma, H.; Liang, X.; Nishioka, H.; Matsunaga, D.; Liu, M.; Komiyama, M. *Nat. Protoc.* **2007**, *2*, 203.
(14) Uno, S.; Dohno, C.; Bittermann, H.; Malinovskii, V. L.; Häner, R.; Nakatani, K. *Angew. Chem., Int. Ed.* **2009**, *48*, 7362.
(15) Bandara, H. M. D.; Burdette, S. C. *Chem. Soc. Rev.* **2012**, *41*, 1809.
(16) Terazima, M. *Phys. Chem. Chem. Phys.* **2006**, *8*, 545.
(17) Nakasone, Y.; Eitoku, T.; Matsuoka, D.; Tokutomi, S.; Terazima, M. *Biophys. J.* **2006**, *91*, 645.
(18) Nakasone, Y.; Ono, T. A.; Ishii, A.; Masuda, S.; Terazima, M. *J. Am. Chem. Soc.* **2007**, *129*, 7028.
(19) Tanaka, K.; Nakasone, Y.; Okajima, K.; Ikeuchi, M.; Tokutomi, S.; Terazima, M. *J. Mol. Biol.* **2011**, *409*, 773.
(20) Nakasone, Y.; Zikihara, K.; Tokutomi, S.; Terazima, M. *Photochem. Photobiol. Sci.* **2013**, *12*, 1171.
(21) Miyamori, T.; Nakasone, Y.; Hitomi, K.; Christie, J. M.; Getzoff, E. D.; Terazima, M. *Photochem. Photobiol. Sci.* **2015**, *14*, 995.
(22) McQuarrie, D. A.; Simon, J. D. In *Physical Chemistry: A Molecular Approach*; University Science Books: Sausalito, CA, 1997.
(23) Von Smoluchowski, M. *Phys. Chem.* **1917**, *92*, 156.
(24) Wyer, J. A.; Kristensen, M. B.; Jones, N. C.; Hoffmann, S. V.; Nielsen, S. B. *Phys. Chem. Chem. Phys.* **2014**, *16*, 18827.
(25) Carrillo-Nava, E.; Mejía-Radillo, Y.; Hinz, H.-J. *Biochemistry* **2008**, *47*, 13153.
(26) Zuo, E. T.; Tanious, F. A.; Wilson, W. D.; Zon, G.; Tan, G. S.; Wartell, R. M. *Biochemistry* **1990**, *29*, 4446.
(27) Wang, S.; Friedman, A. E.; Kool, E. T. *Biochemistry* **1995**, *34*, 9774.
(28) Paiva, A. M.; Sheardy, R. D. *J. Am. Chem. Soc.* **2005**, *127*, 5581.
(29) Gotoh, M.; Hasegawa, Y.; Shinohara, Y.; Shimizu, M.; Tosu, M. *DNA Res.* **1995**, *2*, 285.
(30) Cussler, E. L. *Diffusion*; Cambridge University Press: Cambridge, UK, 1994.
(31) Tyrrell, H. J. V. *Diffusion in Liquids*; Butterworth & Co.: London, 1984.
(32) Yan, Y.; Wang, X.; Chen, J. I. L.; Ginger, D. S. *J. Am. Chem. Soc.* **2013**, *135*, 8382.
(33) Pörschke, D. *Mol. Biol., Biochem. Biophys.* **1977**, *24*, 191.
(34) Craig, M. E.; Crothers, D. M.; Doty, P. *J. Mol. Biol.* **1971**, *62*, 383.

DOI: 10.1021/jacs.6b02525
J. Am. Chem. Soc. 2016, 138, 9001−9004